Mutations in Eml1 lead to ectopic progenitors and neuronal heterotopia in mouse and human

Michel Kielar*, Françoise Phan Dinh Tuy*, Sara Bizzotto*, Cécile Lebrand*, Camino de Juan, Karine Poirier, Renske Oegema, Grazia Maria Mancini, Nadia Bahi-Buisson, Robert Olaso, Anne Gaelle Le Moing, Katia Boutourlinsky, Dominique Boucher, Wassila Carpentier, Patrick Berquin, Jean-François Deleuze, Richard Belvindrah, Victor Borrell, Egbert Welker, Jamel Chelly, Alexandre Croquelois#, Fiona Francis#

SUPPLEMENTARY INFORMATION

Nature Neuroscience: doi:10.1038/nn.3729

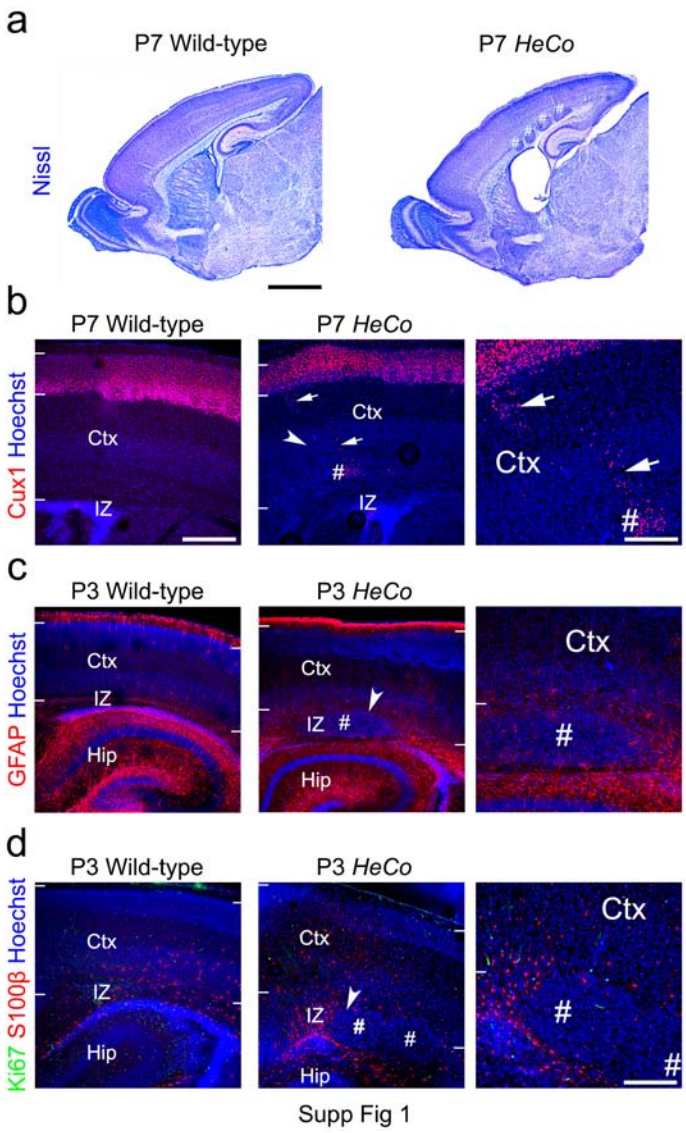

Supplementary Figure 1 Characterization of the heterotopia in postnatal stages in *HeCo* brains. **(a)** Sagittal view of Nissl stained P7 mouse brain. Note the presence of neuronal clusters in *HeCo* cortex compared to wild-type. The clusters are wrapped in the subcortical white matter indicating a discontinuous shaped heterotopia along the rostro-caudal axis. (**b**) Cux1 immunohistochemistry at P7 demonstrating columns of superficial layer neurons (arrows) migrating between the heterotopia (#) and the cortex layer II-IV in *HeCo* brains. (**c**) GFAP labeling and (**d**) S100β/Ki-67 co-labeling at P3 showing subpopulations of glial cells around but rarely inside the heterotopia (#). Far right, higher power views. Cell nuclei of coronal brain sections were counterstained with Hoechst. Scale bars, 2 mm (**a**), 400µm (**b-d**, left and center), 200 µm (**b,c,** far right), 100 µm (**d,** far right).

Nature Neuroscience: doi:10.1038/nn.3729

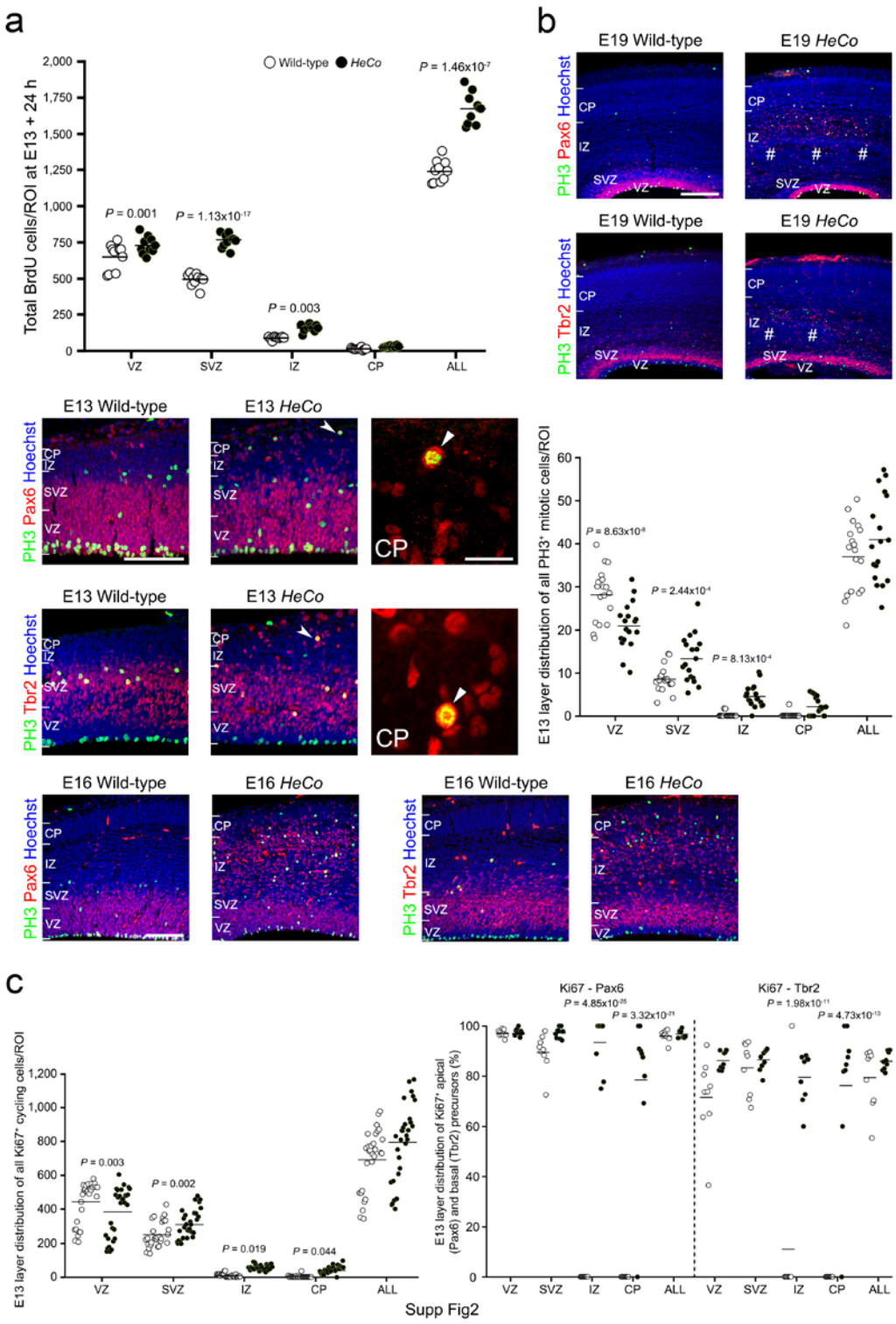

Supplementary Figure 2 Altered distribution of dividing apical and basal progenitors in the IZ and CP of *HeCo* mice. **(a)** After a 24 h BrdU pulse the total number of BrdU$^+$ progenitors is increased in the germinal zones as well as in the IZ (**a**, 3 sections/animal n=3 per genotype, MFA 1 d.f., VZ, p= 0.001, *F*=11.862, SVZ, p= 1.13 x 10^{-17}, *F*=138.703, IZ, p= 0.003, *F*=9.454, CP, p=0.441 *F*=0.601; unpaired *t*-test ALL layers, p=1.46 x 10^{-7}, d.f. 14.481, t=-9.424). (**b**) PH3/Pax6 and PH3/Tbr2 stainings at E19 showing proliferating apical and basal progenitors largely excluded from the heterotopia (#).The distribution of PH3 progenitors was altered at E13 in *HeCo* (decrease VZ, increase SVZ/IZ, 3 sections/animal n=6/genotype, MFA 1 d.f., VZ, p=8.63 x 10^{-8} *F*=32.031, SVZ, p=2.44 x 10^{-4} *F*=14.198, IZ, p=8.13 x 10^{-4} *F*=11.732, CP, p=0.117 *F*=2.495; unpaired *t*-test 32.878

Nature Neuroscience: doi:10.1038/nn.3729

d.f., ALL layers, p=0.202 *t*=-1.303). Overall numbers were not different. Both apical Pax6^{+} and basal Tbr2^{+} progenitors divide ectopically (3 sections/animal n=3/genotype). (**c**) At E13 the distribution of Ki-67^{+} cycling cells is altered in *HeCo* brains (MFA p=0.003 VZ, p=0.002 SVZ, p=0.019 IZ, p=0.044 CP. t-test p=0.065 All, MFA d.f.=1, F=8.931 VZ, F=9.592 SVZ, F=5.550 IZ, F=4.118 CP. t-test d.f. =55.165, t=-1.880; Ki-67/Pax6, Ki-67/Tbr2, 3 sections/animal n=3/genotype, MFA 1 d.f., Pax6^{+}/Ki67^{+}: VZ, p=0.927 *F*=0.008, SVZ, p=0.170 *F*=1.926, IZ, p= 4.85 x 10^{-25} *F*=279.554, CP, p= 3.32 x 10^{-21} *F*=196.991; unpaired *t*-test 11.397 d.f., ALL layers, p=0.366 *t*=-0.941; Tbr2^{+}/Ki67^{+}: VZ, p=0.089 *F*=2.973, SVZ, p=0.704 *F*=0.145, IZ, 1.98 x 10^{-11} *F*=65.935, CP, p=4.73 x 10^{-13} *F*=81.795; unpaired *t*-test 16 d.f., ALL layers, p=0.141 *t*=-1.547). Scale bars 200 μm (E19), 100 μm (E13 and E16) and 20 μm (E13 far right).

Nature Neuroscience: doi:10.1038/nn.3729

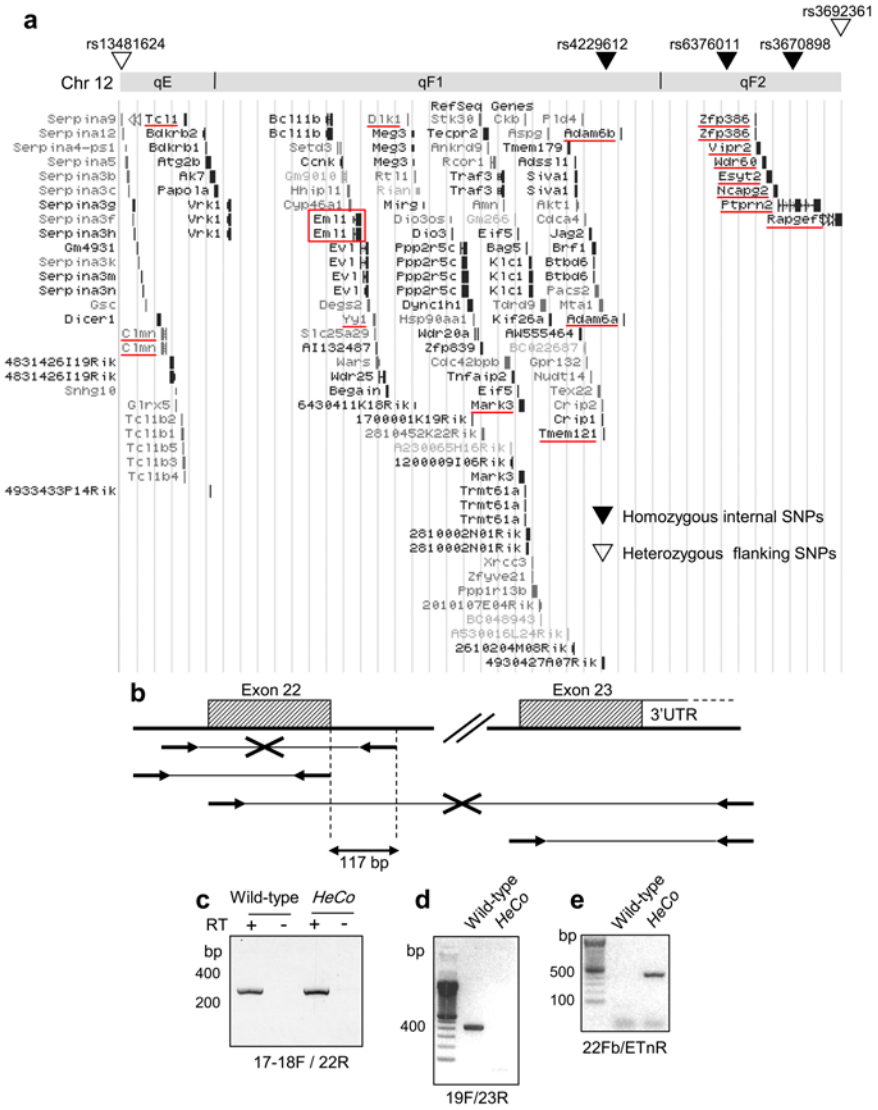

Supplementary Figure 3 Schema of the 13.7 Mb *HeCo* candidate region and analysis of *Eml*1 in WT and *HeCo* transcripts and DNAs. (**a**) Schema of the chromosomal region identified during the first round of genotyping with key SNPs with Refseq genes indicated (captured image from Genome Browser, http://genome.ucsc.edu/; assembly NCBI37/mm9, July 2007). This region shows synteny with human chromosomes 14q and 7q. *Eml*1 is boxed in red. The 15 genes initially sequenced which showed no mutations are underlined. (**b**) Schema showing genomic region containing *Eml*1 exons 22 and 23. PCR products and sequences were identical between WT and *HeCo* except for exon 22 which could not be amplified from *HeCo* DNAs, using primers annealing to nucleotides -85 to -66 upstream and +117 to +96 downstream of exon 22 (➞, primers; ✖, PCRs which failed to give a product). (**c**) RT-PCR between the exon 17-18 boundary and within exon 22 shows identical amplification products from *HeCo* and WT RNAs. RT, reverse transcriptase. (**d**) RT-PCR between exons 19 and 23 shows an amplification product from WT RNAs only. (**e**) A junction fragment between *Eml*1 exon 22 and the ETn 5'LTR is amplified specifically from *HeCo* genomic DNA and not from WT DNA of the same genetic background.

Nature Neuroscience: doi:10.1038/nn.3729

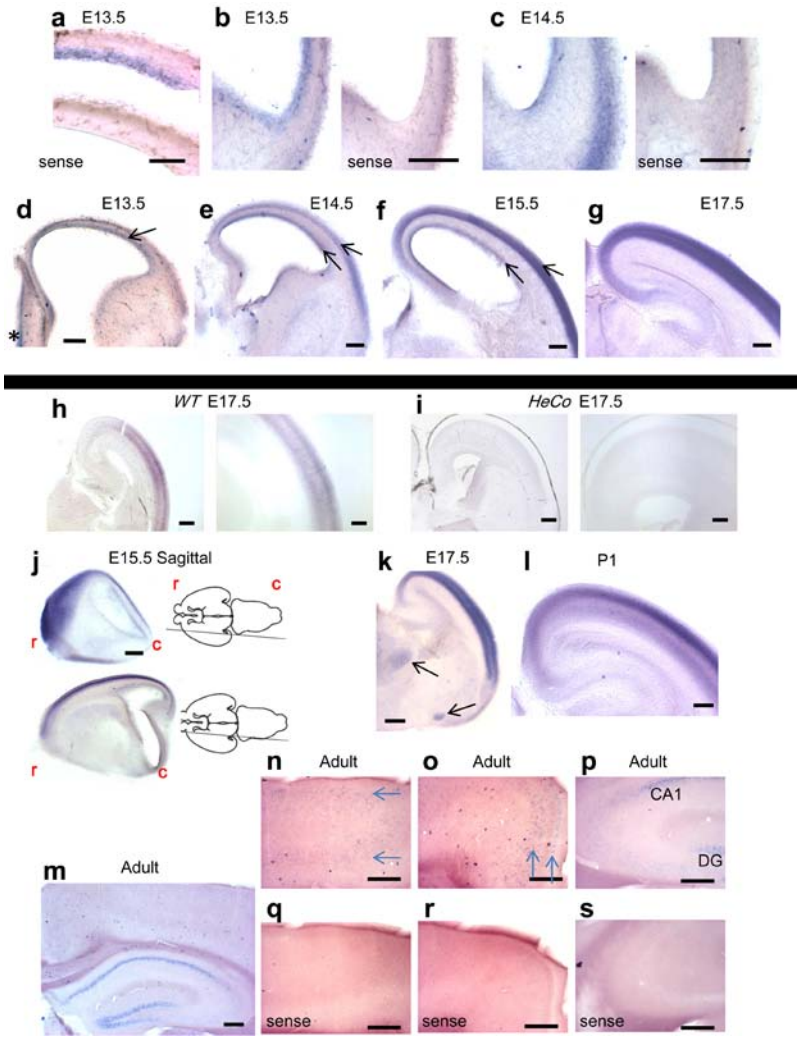

Supplementary Figure 4 *In situ* hybridization of *Eml*1 in the developing mouse brain, additional images. (**a**) Expression in E13.5 dorsal cortex (upper, antisense probe; lower, sense probe). (**b,c**) At E13.5 and E14.5, expression is observed in the VZ at the dorsal-ventral telencephalon boundary but tapers off in ventral telencephalon VZ (left, antisense probe; right, sense probe). (**d-f**) Labeling of *Eml*1 at E13.5, E14.5 and E15.5 in the VZ, or both the VZ and the CP (arrows). A high lateral to low medial gradient is observed. The dorsal thalamic neuroepithelium is also labeled at E13.5 (asterisk). (**g**) Strong two-layered expression in the CP at E17.5 with no further expression in the VZ. Faint expression in the hippocampus. (**h,i**) No *Eml*1 transcript is detected in the *HeCo* developing brain at E17.5 (**i**) compared to WT sections (**h**). (**j**) Strong rostral labeling of *Eml*1 at E15.5, particularly in more lateral regions (upper). On the right are schematized the levels of the sections shown on the left according to *The Mouse Brain in Stereotaxic Coordinates* (Paxinos and Franklin, 2001). r, rostral; c, caudal. (**k**) Thalamic nuclei (upper arrow) and the lateral olfactory tract nucleus (lower arrow) are labeled at E17.5. (**l**) At P1 the expression resembles E17.5, with a stronger expression in superficial layers II and III and a lower expression in deeper layers. (**m**) Expression continues in the adult in some cells of the isocortex, and in CA1 pyramidal and dentate gyrus cells of the hippocampus. (**n-s**) Antisense (**n-p**) and sense (**q-s**) probes hybridized to adjacent mouse adult cortex sections. Faint labeling is observed in superficial and deeper layers of the somatosensorial cortex (**n,** arrows) and in the cingulate cortex (**o**, arrows). Labeling in the CA1 and dentate gyrus (DG) regions of the hippocampus, and little labeling in the CA3 region (**p**). Coronal sections except in (**j**)**,** sagittal. Scale bars, 400 µm (**g,h-left,i-left,j,n-s,m**), 200 µm (**b-f,h-right,i-right,k,l**) and 100 µm (**a**).

Nature Neuroscience: doi:10.1038/nn.3729

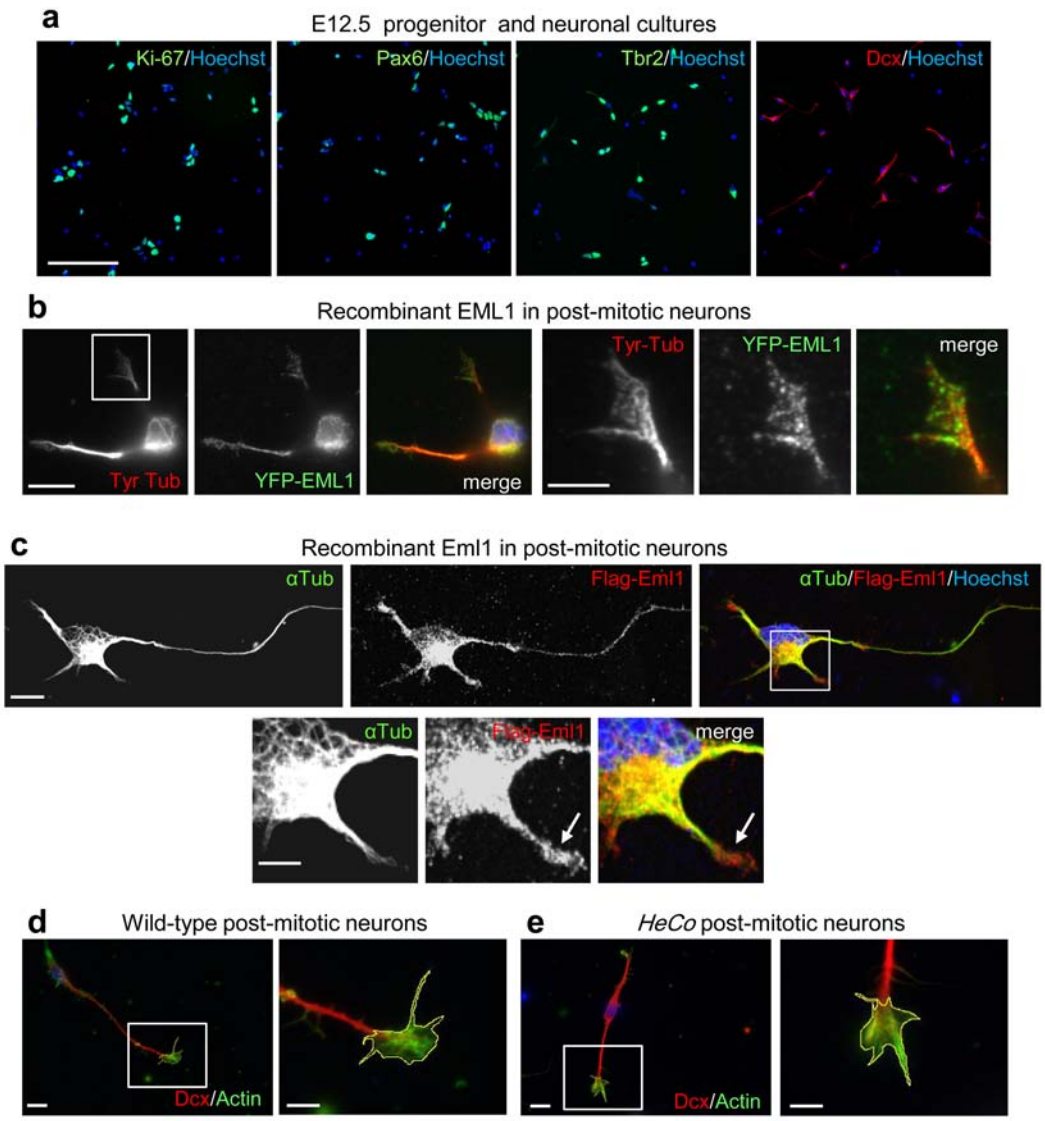

Supplementary Figure 5 Characterization of mixed progenitor and neuronal cultures and recombinant Eml1 in neuronal progenitors. (**a**) Ki-67, Pax6, Tbr2 and Dcx immunolabelings of cultures derived from WT E12.5 dissociated cortex and fixed after 1 DIV. (**b**) YFP-EML1 partially colocalizes with tyrosinated tubulin in perinuclear regions. Punctate labeling aligns with MTs in a growth cone (**b, right**), where little co-localization is observed. (**c**) Flag-Eml1 puncta in a neuron, partially co-localizing with MTs traversing the nucleus and accumulating in growth cones (**c-lower,** arrow, enlargement of the boxed area). (confocal images). (**d-e**) Dcx and phalloidin (detecting F-actin) double labelings. No obvious differences were observed in neuron morphologies and there were similar proportions of monopolar, bipolar and multipolar neurons present in WT and *HeCo* cultures. Growth cones were assessed on cells with relatively uniform morphologies, with a predominant neurite (length between 2 and 4 somal lengths) tipped with a main growth cone. Selection was performed in the Dcx channel, to avoid biased cell selection on the basis of growth cone size. Image J was used to draw around the phalloidin labeling and calculate the surface area and perimeter of growth cones (3 measures for each growth cone; at least 10 cells analyzed in 3 cultures from each genotype, n= 43 for WT and 45 for *HeCo*). A representative growth cone from each genotype is shown. No significant differences were observed in mean surface areas (data not shown). Scale bars, 100 µm (**a**), 10 µm (**b-left,c-upper,d-left,e-left**) and 5 µm (**b-right,c-lower,d-right,e-right**).

Nature Neuroscience: doi:10.1038/nn.3729

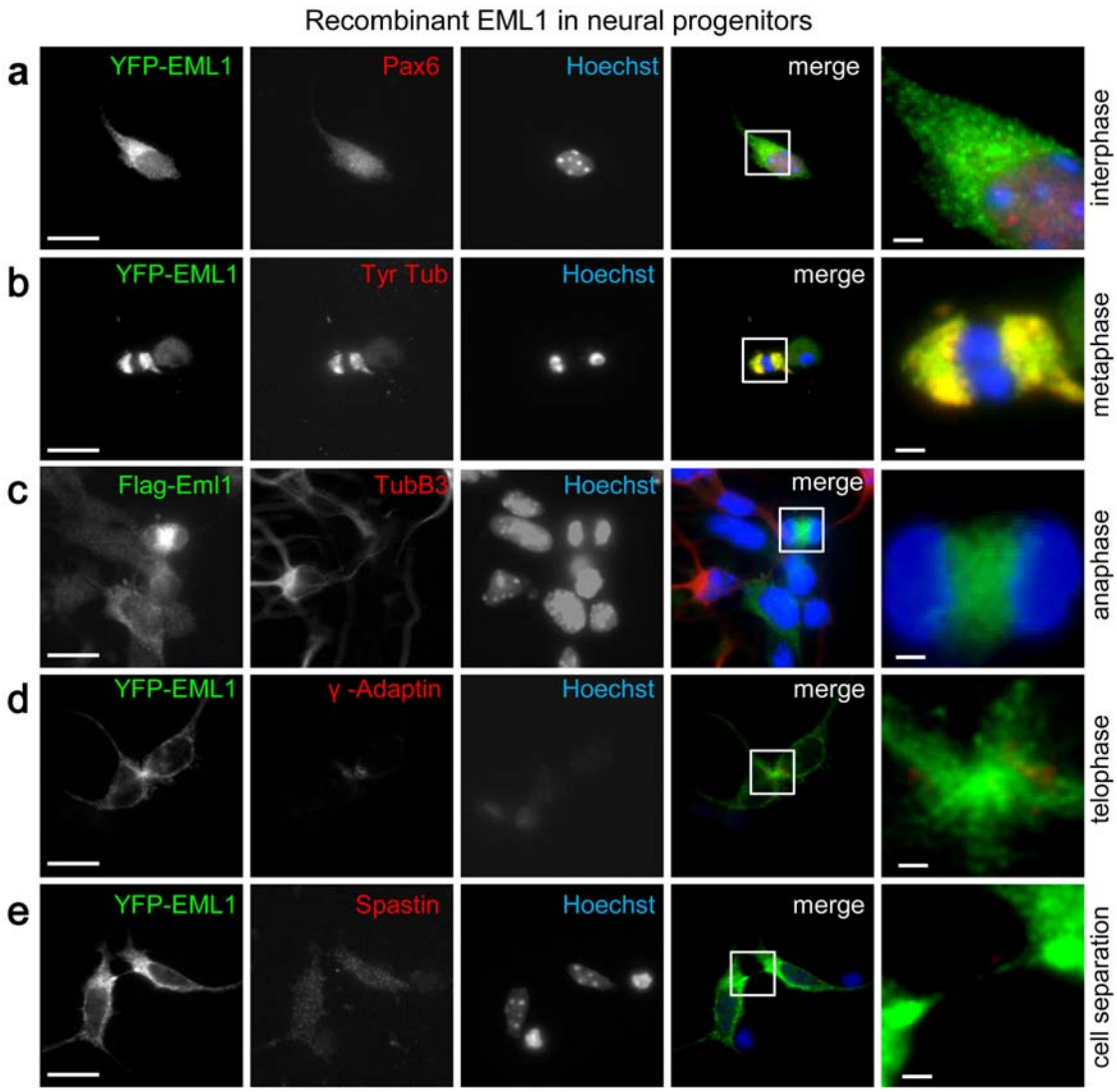

Supplementary Figure 6 Recombinant Eml1 in dissociated neuronal progenitors. (**a**) In neuronal progenitors in interphase YFP-EML1 is distributed throughout the cell in the form of puncta. Co-labeling with Pax6 and Hoechst. (**b-e**) Recombinant YFP-EML1 or Flag-Eml1 in neuronal progenitors at other stages of the cell cycle. Co-labeling with tyrosinated tubulin (**b**), TubB3 (**c**), γ adaptin (**d**), and spastin (**e**). The antibody to spastin gave no specific labeling. In metaphase YFP-EML1 is ubiquitously distributed. From anaphase, early telophase to cytokinesis, an enrichment of YFP-EML1 is observed at the midzone and surrounding region (**c-e**). **a-e**, far right, higher magnifications of boxed areas. In the absence of antibodies detecting Eml1 specifically in neuronal cells, we have not yet been able to compare these subcellular localizations to that of the endogenous protein. Scale bars, 8 µm (**a-e**) and 1 µm (**a-e**, boxed area far right).

Nature Neuroscience: doi:10.1038/nn.3729

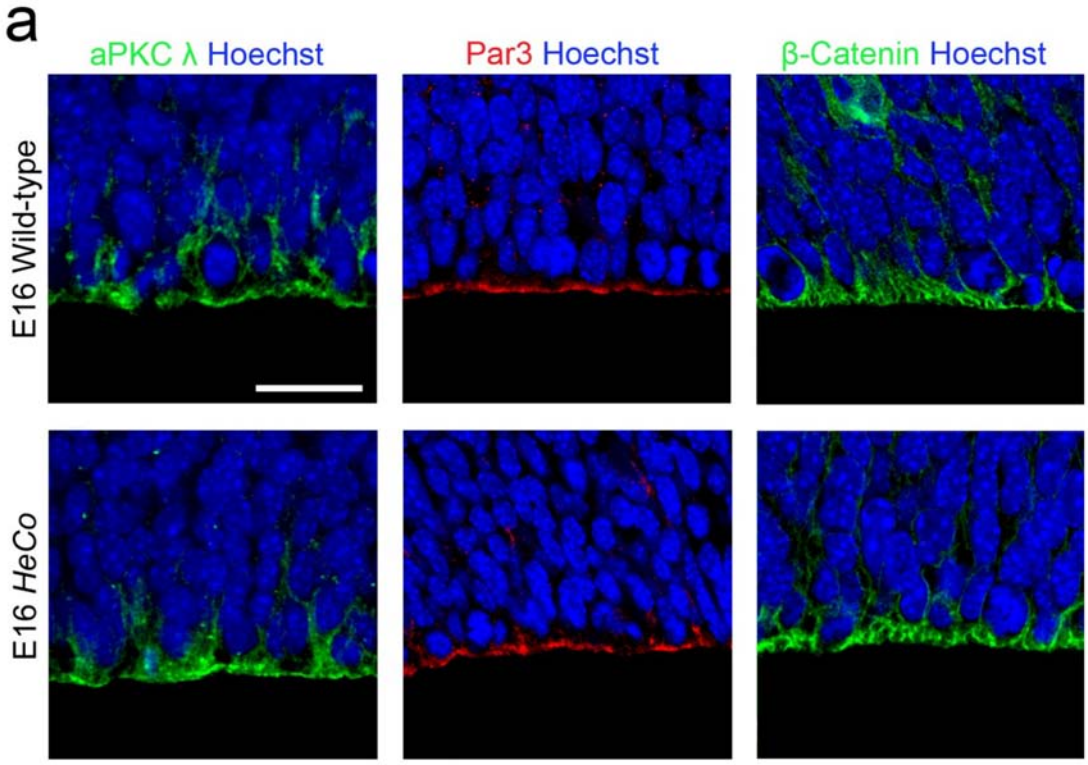

Supplementary Figure 7 (a) Ventricular lining markers in WT versus *HeCo* E16 brains. No differences are observed with αPKCλ, Par3 and β-catenin markers. Apparently normal RGC endfeet at the ventricle lining are observed in *HeCo* brains. β-catenin labeling, as at E13 (Figure 6), reveals typical honeycomb apical membrane structure. Scale bar, 20 µm.

Nature Neuroscience: doi:10.1038/nn.3729

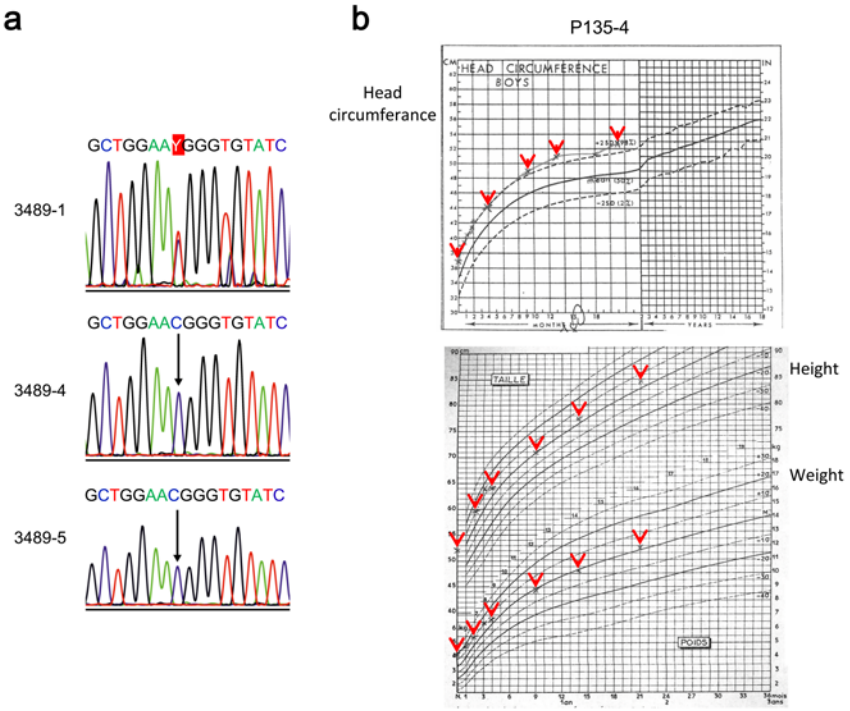

c

	P135-3	P135-4	P135-5	3489-4
Birth	37 cm (+2.5 SD)	37 cm (+2.5 SD)	37.5 cm (+2.5 SD)	42.8 cm (1 week*) (+6 SD)
1 year	51 cm (+2.5 SD)	50.5 cm (+2.5 SD)	51 cm (+2.5 SD)	51.5 cm (+2.5 SD)
Later	55 cm (10 yrs) +2 SD (95th percentile)	53 cm (2 yrs) (+2.5 SD)		57.5 cm (7 years) (+3.3 SD)

+2.5 SD values correspond to ≥ 98th percentile
* At time of drainage related to hydrocephaly

Supplementary Figure 8 Sequence of W225R mutation and anthropometric measurements in patients. (**a**) Sanger sequence confirmation of W225R mutation in family 3489. A heterozygous mutation is observed in the father (3489-1) and homozygote mutations in the two affected sibs. (**b**) As shown in the curves for P135-4, a head circumference greater than (or equal to) the 98th percentile (+2.5 SD) was noted from birth. Height and weight (normal range) are also shown for comparison. (**c**) Anthropometric measurements for children from the P135 and 3489 families. The three P135 children exhibited almost identical macrocephaly from birth, with normal height and weight. Patient 3489-4 suffered from hydrocephaly at birth and was treated by a ventriculoperitoneal drain in the first week. Case 3489-5 presented with hydrocephalus at prenatal ultrasound.

Nature Neuroscience: doi:10.1038/nn.3729

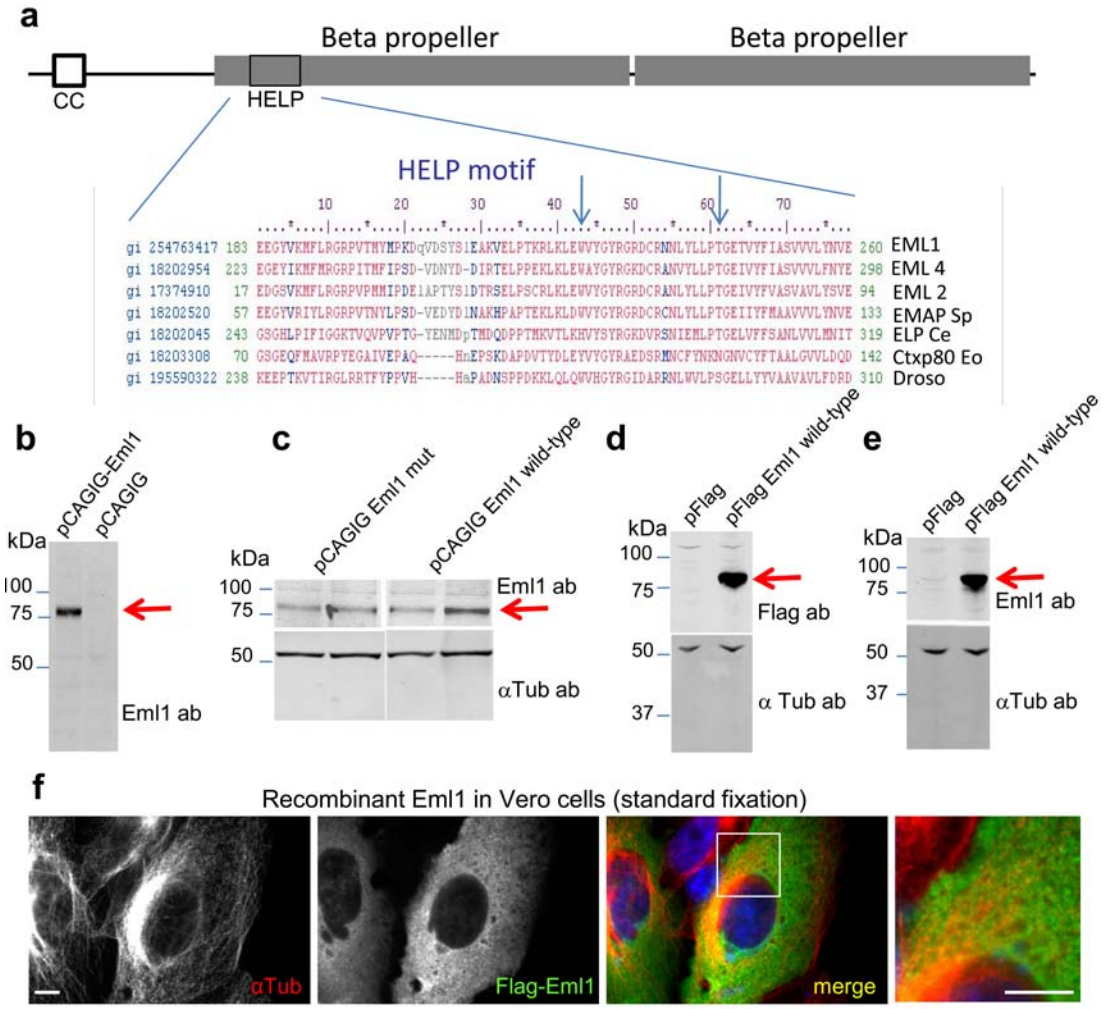

Supplementary Figure 9 Functional domains of EML1, sequence of the HELP domain and expression of recombinant Eml1. **(a)** Predicted domains of the Eml1 protein. Eml1 (814 aa, Uniprot Q05BC3-1) contains a conserved HELP domain in its N terminus (aa 183-259). Other domains, CC, coiled-coil; beta propeller regions containing WD40 motifs. The HELP domain is shown from human proteins EML1, 4, 2, the purple sea urchin *Strongylocentrotus purpuratus* (EMAP Sp), the ELP protein from *Caenorhabditis elegans* (ELP Ce), ciliary WD repeat-containing protein Ctxp80 from the protist *Euplotes octocarinatus* (Ctpx Eo) and *Drosophila melanogaster* DCX-EMAP (Droso). The mutated threonine residue (T243) is conserved in mammalian EML1, 2 and 4, as well as in ELP Ce and EMAP Sp, other family members contain a serine (Droso and EML3) or an asparagine (Ctxp80), suggesting that a polar aa is important at this position (http://www.ncbi.nlm.nih.gov/Structure/cdd/cdd.shtml). The mutated tryptophan residue (W225) is conserved in mammalian EML1, 2 and 4, as well as in EMAP Sp, and Drosophila EMAP. (**b-e**) Western blot expression of transfected recombinant proteins in non-neuronal cells. (**b**) Untagged Eml1 expressed from pCAGIG vector, detected with an antibody to Eml1. (**c**) WT Eml1 protein compared to mutated T243A Eml1 (extracts from two different transfection experiments for each plasmid, control with an antibody to α-tubulin). (**d**) Flag-Eml1 expressed from pNter3xFLAG-CMV vector, detected with an antibody to Flag. (**e**) Same construct detected with an antibody to Eml1. Western blots also confirmed soluble and non-soluble fractions of the recombinant protein (not shown). Western blot analyses to characterize endogenous normal and mutant proteins in mouse brain and human fibroblasts were unsuccessful due to the lack of specificity of different antibodies to Eml1 tested in these cells. (**f**) Vero cells transfected with Flag-Eml1 constructs and fixed with PFA, without detergent extraction. Flag-Eml1 shows a largely cytoplasmic labeling not resembling the MT network. Right, higher magnification of the boxed region. Scale bar, 5 µm (**f-left and right**).

Nature Neuroscience: doi:10.1038/nn.3729

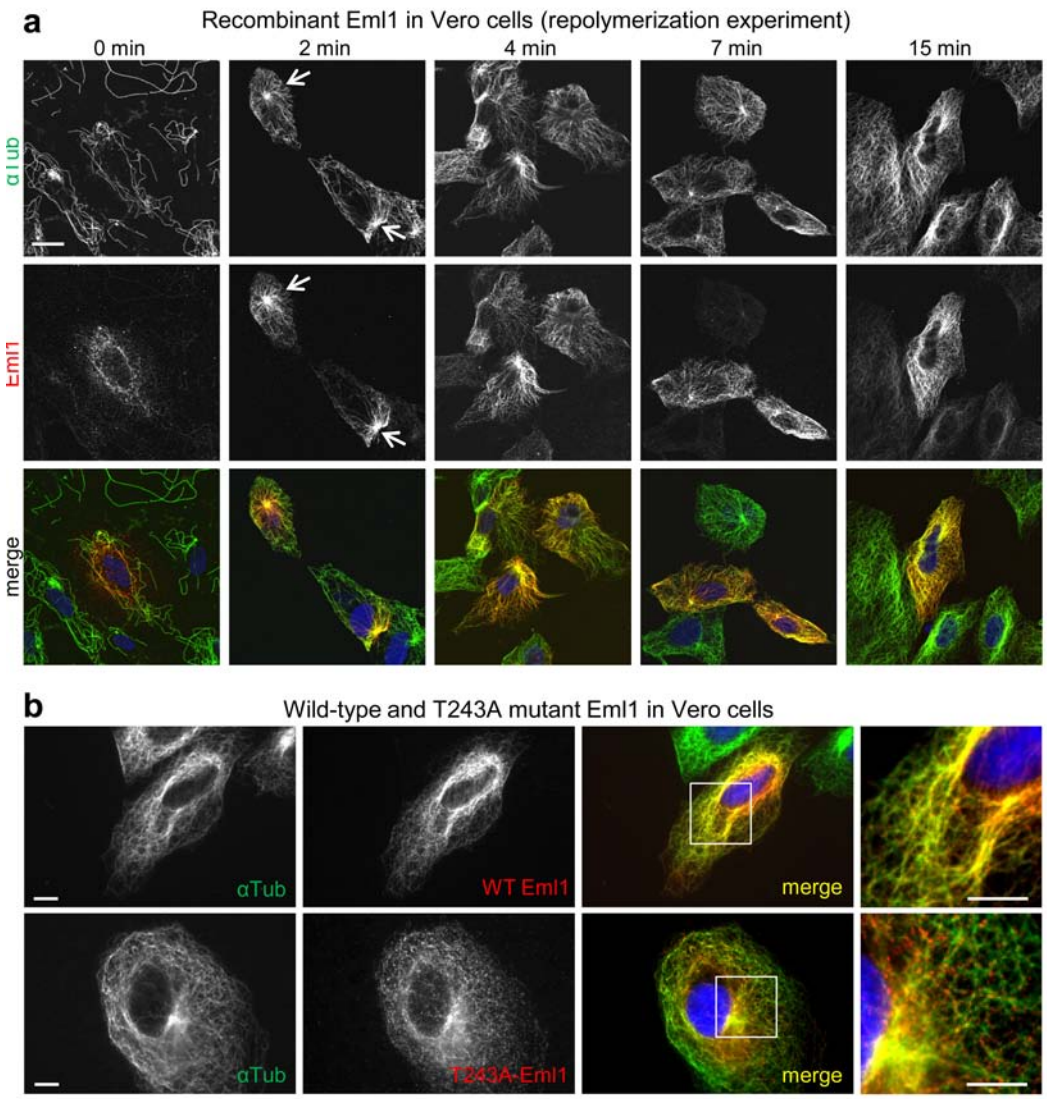

Supplementary Figure 10 Eml1 association with MTs in re-polymerization experiment, effect of T243A mutation. (**a**) Cold-treated Vero cells (0 min, after 30 min depolymerization at 4°C) were restored to 37°C for 2, 4, 7 or 15 min as indicated, before detergent extraction and fixation. At 2 min, a strong localization of untagged WT Eml1 is observed at the region of nascent MTs (arrows) and then progressively extends to the overall array of MTs (confocal images). (**b**) Untagged recombinant Eml1 is detected in untreated Vero cells with the antibody to Eml1 after detergent extraction. An MT-association is observed for the WT version (upper row) whereas localization of the T243A mutant protein (lower row) is altered, showing less association with MTs and a more predominant punctate appearance. This result was consistently obtained in multiple experiments. Scale bars, 20 µm (**a, for all images**) and 5 µm (**b, left and right**).

Nature Neuroscience: doi:10.1038/nn.3729

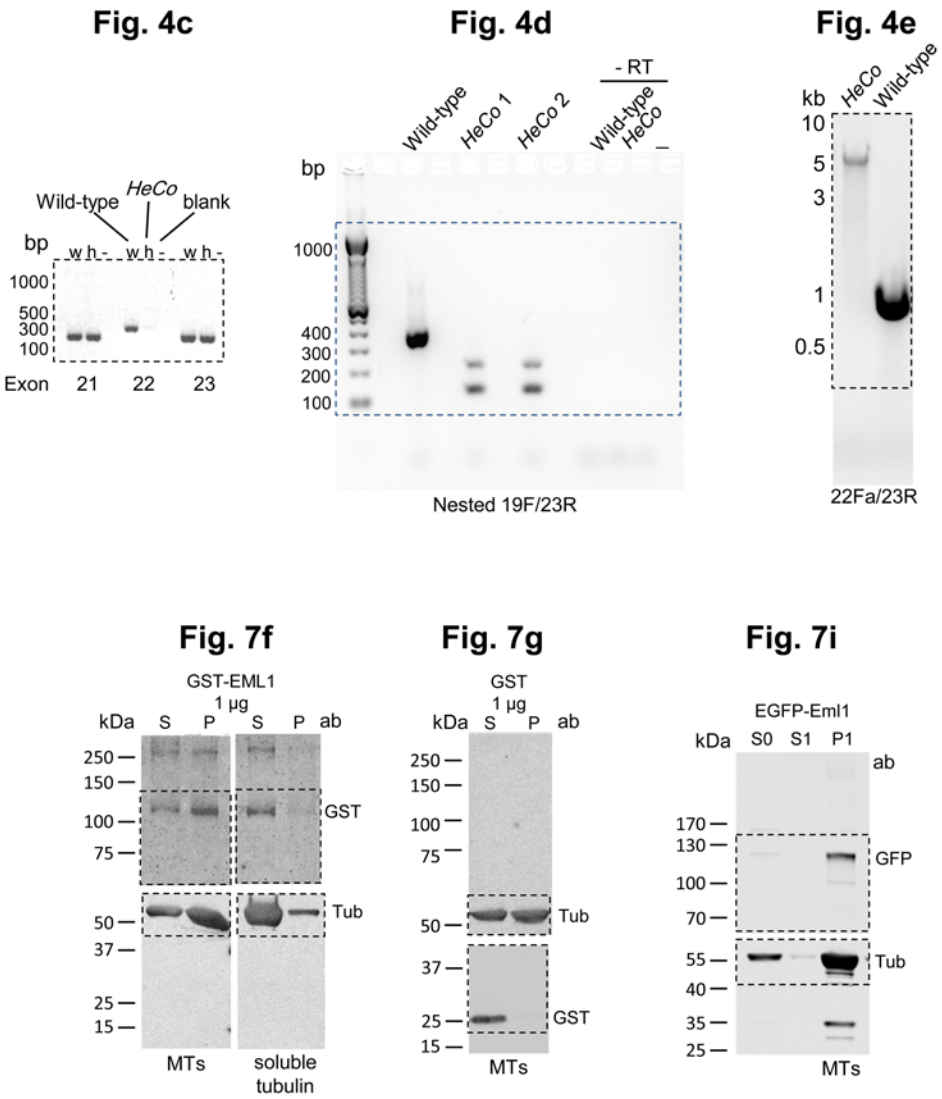

Supplementary Figure 11 Full-length pictures of the gels (Fig. 4c, 4d, 4e) and blots (Fig. 7f, 7g, 7i) presented in the main figures. For Fig.7 blots, to detect αTubulin (Tub) and the protein of interest in the same samples, blots were first cut and then incubated with indicated antibodies (ab).

Nature Neuroscience: doi:10.1038/nn.3729

Supplementary Table 1 Key SNPs and informative individuals in the fine mapping of the *HeCo* mouse candidate region. Heterozygote genotypes are highlighted in grey. SNPs rs4229612, rs6376011, rs3670898 for the first round and SNPs rs29180599, rs6240517 for the second round were found homozygous for the NOR alleles in all F2 affected individuals. After the second round of screening rs29151683 and rs29219055 were identified as flanking markers (underlined). The region was slightly further reduced by the identification of a non-referenced SNP in the *Dlk*1 gene. Non informative genotypes are noted '-'.

		F0 C57 WT	F0 C57 WT	F0 NOR	F2 tree 1								F2 tree 2			
SNP	**nucleotide**	**Tree 1**	**Tree 2**	**HeCo**	**71**	**124**	**160**	**224**	**164**	**250**	**186**	**194**	**368**	**395**	**552**	
rs13481624	105,246,728	CC	-	GG	CG	CG	CG	CG	CG	CG	GG	GG	-			5' boundary (1st round)
rs29151683	106,303,360	AA	-	GG	GG	GG	GG	GG	AG	AG	GG	GG	-			Final 5' boundary (2nd round)
rs29180599	108,884,307	CC	-	AA	AA	AA	AA	AA	AA	AA	AA	AA	-			Internal homozygous (2nd round)
rs6240517	109,744,829	AA	-	GG	GG	GG	GG	GG	GG	GG	GG	GG	-			Internal homozygous (2nd round)
non ref	110,693,217	-	CC	TT	-	-	-	-	-	-	-	-	CT	CT	CT	Final 3' boundary (Dlk1)
rs29219055	110,727,094	-	CC	GG	-	-	-	-	-	-	-	-	CG	CG	CG	3' boundary (2nd round)
rs4229612	114,496,842	GG	-	AA	AA	AA	AA	AA	AA	AA	AA	AA	-			Internal homozygous (1st round)
rs6376011	116,788,762	GG	-	TT	TT	TT	TT	TT	TT	TT	TT	TT	-			Internal homozygous (1st round)
rs3670898	117,956,773	CC	-	GG	GG	GG	GG	GG	GG	GG	GG	GG	-			Internal homozygous (1st round)
rs3692361	118,957,587	TT	-	CC	CC	CC	CC	CC	CC	CC	CT	CT	-			3' boundary (1st round)

Supplementary Table 2 : Primers

qPCR	
mE1utr For1	CACAGACAGCATGCAGCATACA
mE1utr Rev1	CTTCTCGACACCTTCAGACCCTAC
mE1_34 For1	CTCAACAGGAAAGGACCTACCAA
mE1_34 Rev1	GTTGACGGTGGTTCTCAATGG
mHdac3 For1	CGCATCGAGAATCAGAACTCAC
mHdac3 Rev1	TCAAAGATTGTCTGGCGGATC
mAt5g3 For2	GCAGTCTTATCATTGGTTATGCCA
mAt5g3 Rev2	AGAACAGCTGCTGCTTCAGTGA
mErp29 For1	CCTTCCCTTGGACACAGTCACT
mErp29 Rev2	GTCGAACTTCACCAAGACGAACTT
Mouse *Eml1* genomic	
Eml_1F_336	cccatctgccctacatacca
Eml_1R_336	ccgtcagtaaagccatccat
Eml_2AFbis	GCGCAGTGTGTGGGTGA
Eml_cDNA3R	CGCTGACTTGAGCAGTTGAA
Eml_3F	TCATGGGCTGTACGTCACTC
Eml_3R	GAGATTGGTTCAGTGGGTGG
Eml_4F	GGATCGTTCCTGCTGCTATG
Eml_4R	GCTGCTTTGAGAAGTCAGGTG
Eml_5F	CTCAGTACACTGGGCAATGAAG
Eml_5R	GGCTTGACTCATCAAGAGGG
Eml_6F	CACACATGCAAGCACACATC
Eml_6R	TTCCCCACTCAGTCAAGGTC
Eml_6aF(alternative)	CCCTTGTTCCCTTGTCCC
Eml_6aR	TATGAGAACAGCCTCAGGGG
Eml_7F	GTGTTTGCTTTCGGAGCG
Eml_7R	TGGCCACATCTGAAATTTTG
Eml_8F	ATCTTTGGGCCTGTTGAATG
Eml_8R	TGATGCTGAATTCTTTTGGC
Eml_9F	GAAGCTAGGCAGTGTGGATTTC
Eml_9R	ATGTCGCCAGGAGGTTGTC
Eml_10F	TTTATGGTTCCAAGGTAAAGAGAAG
Eml_10R	ATGCCTTGAGAAAGGCTGG
Eml_11F	TCGTGTTGGTCCCACTTG
Eml_11R	GCAGGTCTTAGGCAGGGTC
Eml_12F	CTTGAGAGACTCAGTGCCCC
Eml_12R	CTCAGCGCTCCCTTATAACC
Eml_13F	CAAATAAAAGGCTGTCTTCGG
Eml_13R	GGTTGTCCTGTTCGTAACTCC
Eml_14F	CAAACTGAAGTGGGTTTCGG
Eml_14R	GAATCCAAACGGCCAGC
Eml_15-16F	GCCTCGCTTGCACAGTAAGT
Eml_15-16R	TGTTAATTCATACAAAGATATATCCCA
Eml_17F	GAGTCTGAGAAGAGCAGGGC
Eml_17R	CTCAGCCGTCTAACTGCTCC
Eml_18F	TCTGTAGAGAAAGCTGTGGGG
Eml_18R	GTTCGCTGTCTAGTGAGCCC
Eml_19-20F	CCAGCCTTTCCTCTTACGAC
Eml_19-20R	CCCATGGGAATGTCAGAGTG
Eml_21F	AGGACTCTGCCTGACTCCAG
Eml_21R	TGGAGAAGGTATGGTCTCGG
Eml_22F	TGAAGGTGGATTTCTGTCCC
Eml_22R	TTAACAGGGTCATATGCAGGC
Eml_23F	GACTGATTTAGTGCTCGGGG
Eml_23R	GAAATCACAGTGACCAAGCG
Eml_3utr 1F	TGCAGTGGCGAGTCATTTAG
Eml_3utr 1R	TTAACCAGGGAGAGCACAGC
Eml_3utr 2F	GCTTTCCTTGGCCATGTATC
Eml_3utr 2R	TGTATGCTGCATGCTGTCTG
Eml_3utr 3F	CCTTTGAGGCTCTGGGTGTA
Eml_3utr 3R	GGGAACAGGATGTAGTGTGGA

PCR and RT-PCR region of mouse Eml1 exons 17-23	
Eml_22Fbis1	AGAGATGCAGGGCTTCTCAG
Eml_22Rbis	GGAACTGTGAGCACGGGTAT
Eml_22Fter	CCGATGGGACAGACATCAAC
Eml_RT17-18F	ACTGACTGGGAGGTGGTTTG
Eml_19F	TGGAGTTACCGACAATGGAAG
RTEml_23R	AGGAAGTCCACGTTGGTGAC
Eml_Nested 19F	ACACGAGTTGGCAAGTGCTC
Eml_Nested 23R	CCACTGTAGATGTGGCTTGG
Eml_RT19-20F	CAAGTGCTCCGGCCATTC
qPCR N2a	
Em1_RT17-18F	ACTGACTGGGAGGTGGTTTG
Em1_RT20R	GTCCAAGTGGGTGATGAAGC
Etn	
ETnR	CCGCTCGAGCTGTAAGAG
ETnSD-7R	GAGACTACATCTCCTCCTTG
ETnF2	CTCGAGCGGCCTTCTCAGTC
ETnSD261R	TGAGAAGGCCGCTCGAGTTG

Human EML1 primers (according to NCBI RefSeq NM_004434.2)

Exon	Forward 5'-3'	Reverse 5'-3'	Amplicon(bp)
1	AGCTCAGTGTGTGGTGAGCG	CCCCGCGGCTCCAACACAAT	320
2	GCTTAAGAGCAGTATCTGTAGTCCG	TTAAAGAGCACAATGTGTTTGC	406
3	GGTAACATGAGTGATGGGTA	CACACTGTGGTTTTAGCCAG	543
4*	GTGCGTCCTGCAATTTACTG	CACTGGACAAGACCTTGAAGC	254
5	GACGTTCTATGTATATATTT	TGTTTGATTAGTCCTATAAA	380
6	GGCTTTGGGGTCTGAAGTG	AAGCTCCTGTGTGTCCAAGG	216
7	CAAAAGCAAACAAGATGCAAAC	GGAATGATAAGTTGGTTCTCCTG	564
8	CTGCATGCCTTTTGGGG	TGACCGTGTTCTGCTAATGC	505
9	TTGAAATGGTATTTTCCCAGC	CACCCTGCCACACAATAAGTC	505
10	GTCCGAGTTACTGCCCAAG	CCCCTCTTCAACCCTGAG	281
11	GTCTCAAAAGCAATGGATGAG	ACCACTATGCCAGGGCG	306
12	TTTGTGGCTCACATTTTACTTG	GATCCCAAGGGATTGTGTTG	326
13	CAGAAATGCAAGGTGTGCAG	TCTCCGCTTTTCCTCTGTTC	450
14	ATTGCAATGATGTGCTCACG	TGTGATTTCACCTAAACAATTTT	389
15-16	AAGTGTTTTGAATGACTGAGCTAAC	AACATTTGCTTTGGGACAAC	706
17	GCCCTAAGGAATTAGAAGTGTG	GCCTGTTCCTGGGGAAATAG	262
18	TAAGCAAATTCTGAGTATTT	CATGGGCTCACTTATAAGTG	500
19-20	GGTGGCAGCTACCGTTATCC	GGAGGTGGGTTCTCACAGAG	475
21	CCAGGAAGGGCTCTGTACC	TGGTGACCATGAGACTCCG	294
22	TCATGTTCAGGACCGTTCAG	TAGTCTCCAAACAGGTCGGG	297
23	ATTCAAGCACTTTCCCATCC	CTGAAGTGATCTGTCCTTTTAGG	657

* exon 4 is present in the mRNA NM_001008707 not in the mRNA NM_004434.
Human and mouse genes have the same structure overall with some distinct alternative exons.